Detailed Performance Analysis of a 10 kW Dish/Stirling System

Article *in* Journal of Solar Energy Engineering · February 2008

DOI: 10.1115/1.2807191 · Source: DLR

7 authors, including:

Alain Ferriere
French National Centre for Scientific Research
48 PUBLICATIONS **992** CITATIONS

SEE PROFILE

W. Reinalter
e-mail: wolfgang.reinalter@dlr.de

S. Ulmer

P. Heller

T. Rauch

German Aerospace Center (DLR),
Institute of Technical Thermodynamics,
Pfaffenwaldring 38-40,
D-70569 Stuttgart, Germany;
Plataforma Solar de Almería (PSA),
04200 Tabernas, Spain

J.-M. Gineste

A. Ferriere

F. Nepveu

PROMES-CNRS Laboratory,
7 rue du Four Solaire,
66120 Font-Romeu, France

Detailed Performance Analysis of a 10 kW Dish/Stirling System

The CNRS-Promes dish/Stirling system was erected in Jun. 2004 as the last of three country reference units built in the "Envirodish" project. It represents the latest development step of the EuroDish system with many improved components. With a measured peak of 11 kW *electrical output power, it is also the best performing system so far. The measurement campaign to determine the optical and thermodynamic efficiency of the system is presented. The optical quality of the concentrator and the energy input to the power conversion unit was measured with a classical flux-mapping system using a Lambertian target and a charge coupled device camera system. An efficiency of the concentrator including the intercept losses of 74.4% could be defined for this particular system. For the thermodynamic analysis all the data necessary for a complete energy balance around the Stirling engine were measured or approximated by calculations. For the given ambient conditions during the tests, a Stirling engine efficiency of 39.4% could be measured. The overall efficiency for the conversion of solar to electric energy was 22.5%.*
[DOI: 10.1115/1.2807191]

Keywords: dish/Stirling system, EuroDish, performance analysis, optical efficiency, thermodynamic efficiency, flux mapping, energy balance

Introduction

The "EuroDish" dish/Stirling system with a nominal power output of 10 kW was developed in a joint European project with the same name from 1998 to 2001 (Fig. 1). In a first step, two prototypes were built during that project and operated since then on the Plataforma Solar de Almería. Two almost identical systems were built later in Italy and India. A second development step was made in the project Envirodish financed by the German Ministry of Environment introducing many improved components to the system and ending with the erection of three "country reference units" in Seville (Spain), Odeillo (France), and Würzburg (Germany). The three systems were erected in 2004 and since then operated continuously by the local partners. Although the systems are now equipped with an integrated data acquisition system and the improvements concerning output power are obvious, it was necessary to carry out a detailed measurement campaign to collect reliable data for the performance analysis of the system. The measurements on the reference unit in Odeillo were carried out in two phases in summer and winter of 2005 of the "Solface" program financed by the European Commission. This article describes the methodology, used equipment, and results of the measurement campaign.

Methodology

The relevant energy flows between the subsystems of a dish/Stirling unit and the typical losses of these components are presented in Fig. 2. The sunlight is reflected by the concentrator toward the focal point. Some parts of the concentrator are shaded by structural elements and the power is reduced also by the reflectance of the mirrors. Only a portion of the concentrated sunlight enters through the aperture of the cavity. Inside the cavity, only a part of the remaining power is directly absorbed by the receiver. Another part is reflected back through the aperture or to the cavity walls where it might be absorbed or reflected again. The hot surfaces inside the cavity cause radiation and convective losses through the aperture and conductive losses through the isolated cavity walls. The thermal power transferred to the receiver is partly converted to mechanical power by the Stirling cycle. The cooling water stream transports the other part of the heat to the air radiators of the Stirling unit. Some additional thermal losses are caused by the warm engine surfaces through radiation and convection. Finally, the generator converts a big part of the mechanical power to electricity and dissipates the residual part into the Stirling engine housing.

Since energy input and output of the Stirling cycle have to be equal for steady state conditions, the principal idea of this campaign was to make precise measurements of the systems optical characteristics, which allows to calculate the input power to the Stirling engine for the given aperture geometry and ambient conditions. This input power must be equal to the sum of the thermal and mechanical output of the Stirling engine measured at the same time, which gives the constraints for necessary assumptions about losses that have to be made since not all energy transfers within the engine can be measured directly.

The optical behavior of the concentrator can be determined with a solar flux measurement system. With this method, the input of concentrated radiation into the cavity and the portion of the radiation hitting directly the receiver can be determined precisely when the direct normal irradiation and the reflectance of the concentrator are known. The optical material properties and the geometries of the cavity and the receiver are known, which allows a good approximation of reflective and thermal losses.

On the output side of the engine, precise electric and thermal power measurements are necessary. Since the generator efficiency is known, the mechanical power of the Stirling engine can be

Contributed by the Solar Energy Engineering Division of ASME for publication in the JOURNAL OF SOLAR ENERGY ENGINEERING. Manuscript received September 21, 2006; final manuscript received September 10, 2007; published online December 28, 2007. Review conducted by Diego Martinez-Plaza. Paper presented at the SolarPaces—13th International Symposium on Concentrating Solar Power and Chemical Energy Technologies 2006.

Fig. 1 The CNRS EuroDish System

deduced. The thermal output of the engine can be measured combining precise temperature and flow measurements of the cooling water to a calorimetric measurement.

Insolation Data Measurement

The exact measurement of the direct normal insolation is crucial for the whole measurement series. It is obtained from an actinometric station placed on top of the Odeillo big solar furnace a few hundred meters away from the dish/Stirling system. The solar part of the station is equipped with three sensors, a normal incident pyrheliometer (EPPLEY) to measure the direct normal insolation (I) and two CM6 (Kipp & Zonen) pyranometers in order to obtain the global horizontal (G) and diffuse horizontal (D) insolation. The sensors are periodically calibrated at the laboratories of Carpantras, which is part of the Météo-France network and in possession of an absolute radiometer on the international radiometric scale. The measurement uncertainties are about 1.5% for the pyrheliometer and 3.5% for the pyranometers [1].

Flux-Mapping System

A flux measuring system for dish/Stirling systems developed by DLR was used to map the flux distributions close to the focal plane. It consists basically of a Lambertian target placed in the beam path, a charge coupled device (CCD) camera, and a computer that controls target positioning and image acquisition. The target is made up of a water-cooled aluminum plate with a plasma-sprayed alumina coating, which is close to ideal diffuse reflection properties. A Peltier-cooled slow-scan CCD camera is mounted in the central hole of the concentrator taking pictures of the illuminated target. The acquired images are automatically processed and evaluated in the image analysis program OPTIMAS®. Image calibration is achieved by calculating the total reflected power coming from the dish and relating it to the integrated gray values measured on the target in the focal plane. This calibration method assumes that the target in the focal plane intercepts all the sunlight reflected by the dish. Simulations for the given case proved that spillage is almost negligible being less than 1% even for bad sunshapes. Error analysis resulted in a calibration uncertainty of ±2.5% and local measurement uncertainties of −2.5% to +8.5% for this measurement system [2,3].

Cooling Power Measurement System

To precisely measure the power evacuated by the cooling system, the change of coolant enthalpy between water inlet and outlet was determined, and the mass flow was measured. A mixing chamber was connected to the outlet and a temperature sensor placed at the outlet of this chamber to guarantee a homogeneous temperature in the outlet stream. At the motor inlet, a proper mixing was assumed due to the short distance between the circulation pump and the motor inlet. Thus, the sensor was simply placed in the center of the inlet water tube.

The sensors used were high precision PT100 1/10 DIN B according IEC751 with an accuracy of ±0.013 K. Their signal was measured with an ICP DAS model I-7033 in four wire configuration with an accuracy of 0.1%. An additional calibration was conducted by adjusting their temperature difference signal to zero with the water pump switched on and the engine in stow position. A noise of 0.05 °C under static conditions was measured.

An electromagnetic flowmeter was selected to determine the mass flow of the coolant. This device is able to measure the flow of conductive liquids regardless of their composition with very high precision. The flowmeter was installed according to the manufacturer's specifications and its inner diameter is the same as the main rectilinear return pipe in order to be in unruliness state. The low liquid temperature and the expansion vessel in the cooling circuit prevent appearance of bubbles.

The Siemens Sitran MAG 3100 with a maximum flow rate of 5000 l/h and the electronic evaluation unit (MAG 6000) has a specified precision of ±0.5%. The calibration report indicates a maximum error of ±0.17% from 25% to 91% of the full scale flow.

The measurements were taken in winter with negative outside temperatures. The cooling mixture used is a standard automotive-type ELAN FLUID D with full protection down to −26 °C. Since the exact composition was not known, a sample was taken and analyzed by the French Laboratoire National d'Essais. The measured heat capacity as function of the temperature had an unexpected high uncertainty of ±4%. The mean density was determined to be 1060 kg/m^3.

Electric Power Measurement System

Measurements of the electric power output of the generator and the consumption of the individual components were performed using a WEIGEL DUW 2.0 power transducer together with the recommended transformers (30/1) for the current measurement inputs. With a true three-phase conversion of the current and voltage inputs, this device guarantees an absolute correct result of the measurements within the accuracy class of ±0.5%. Since the transducer was placed at the output of the Stirling engine's electric circuit and therefore measures the net output, the constant con-

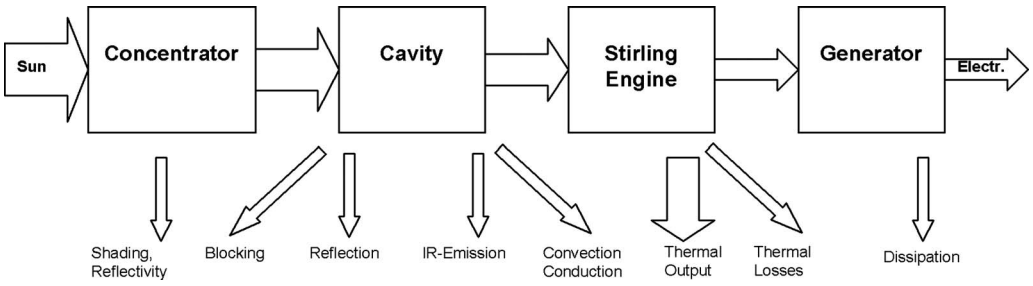

Fig. 2 Energy flow in a dish/Stirling system

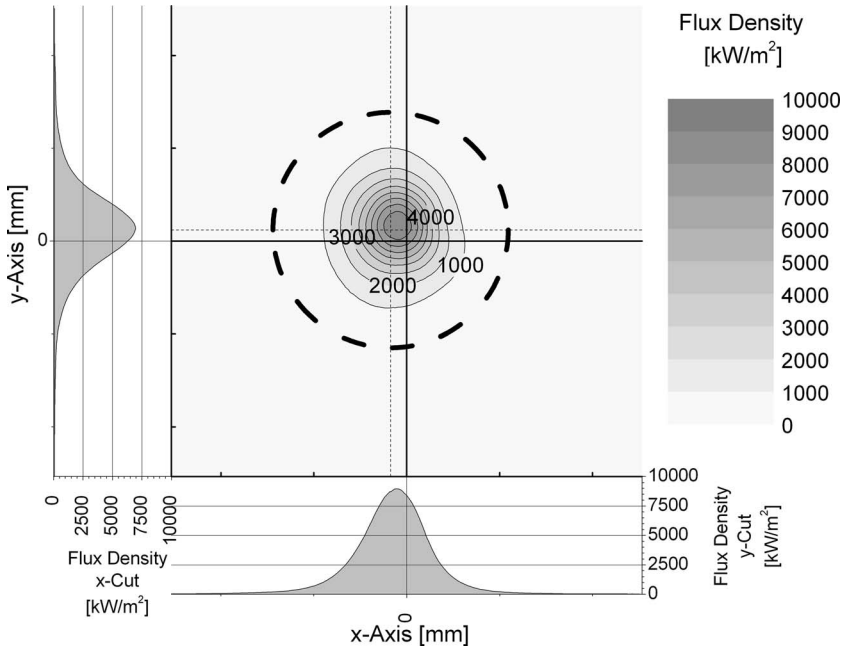

Fig. 3 Normalized flux distribution in the focal plane

sumptions of all individual parasitic loads (water pump, electronic circuit, and cooling fan) had to be measured first using the same equipment. The generator efficiency only changes less than ±0.5% around the specified efficiency of 92.5% for a wide power range and therefore was considered constant for the calculation of shaft power.

Measured Flux Distribution

Flux measurements were performed in the first week of Aug. 2005 in planes perpendicular to the optical axis in steps of 20 mm within a range of ±200 mm around the focal plane. All values were normalized to 1000 W/m^2 of direct normal insolation and 94% mirror reflectance. Figure 3 shows the measured flux distribution in the focal plane. It represents a close to symmetric Gaussian distribution with a peak concentration factor of 9305 suns. The maximum aperture intercept with a diameter of 190 mm (dashed circle) is with 86.8% slightly below the design value of 90%. The position of the focal spot is with $x=-15$ mm and $y=+7$ mm slightly left and high. Figure 4 shows the flux distribution in the absorber plane 120 mm further behind. It is rather inhomogeneous with a considerable peak of 1583 kW/m^2 in the upper part of the receiver (dashed line).

Figure 5 shows the diagrams of peak flux density and aperture intercept depending on the distance to the focal plane. It can be

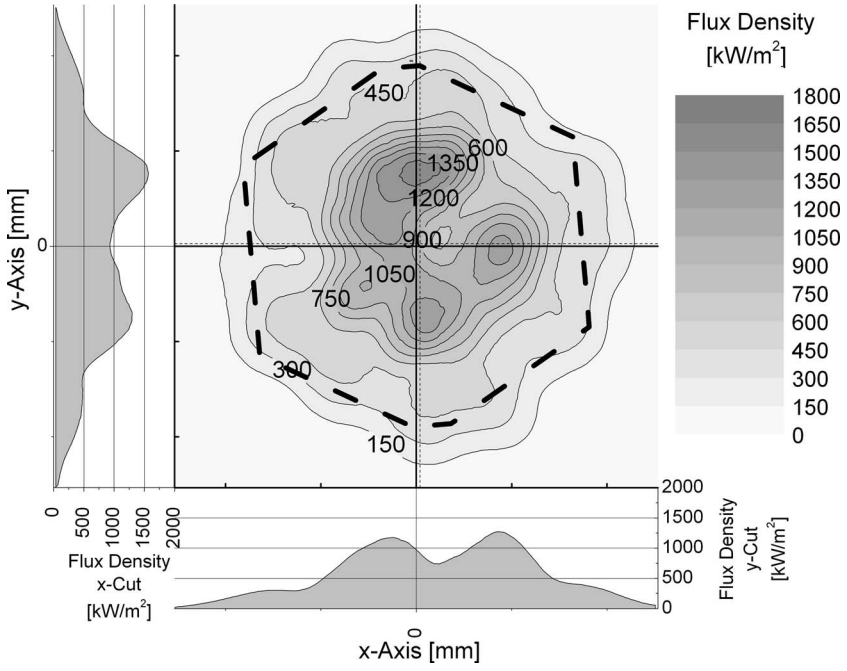

Fig. 4 Normalized flux distribution in the absorber plane

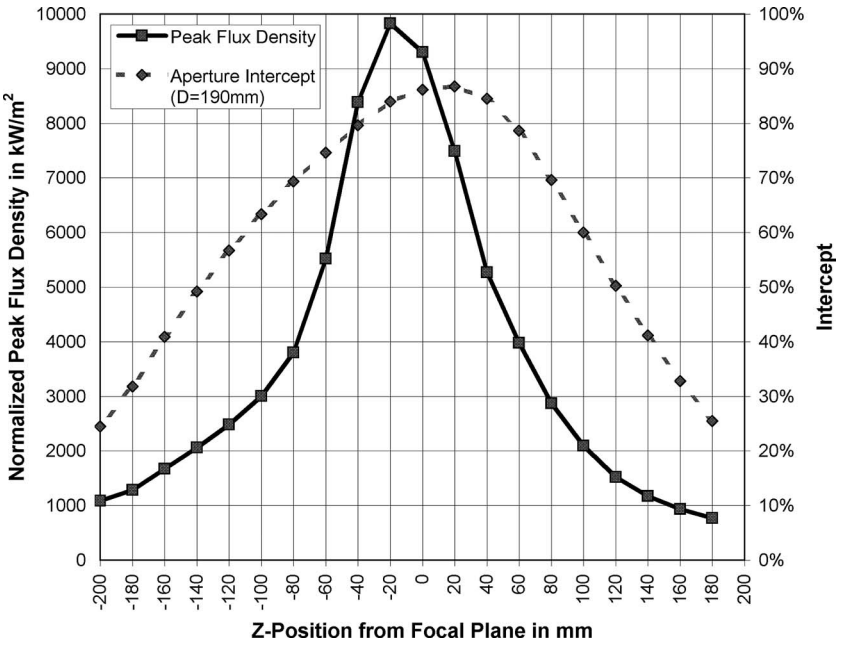

Fig. 5 Peak flux and aperture intercept variation close to the focal plane of the EuroDish

seen that the plane of highest concentration ($z=-20$ mm) is not the plane of highest aperture intercept (between $z=0$ mm and $z=+20$ mm). The focal plane was defined in between, where the 70% radius is smallest (see Fig. 6).

The lines in Fig. 6 show the radii that intercept a certain percentage of the incoming radiation over the distance from the focal plane together with a section of the system's cavity. It can be seen that, with the receiver mounted in this position, about 10% of the total radiation hits the front protection, another 5% hits the aperture ring, and 85% enters the cavity. About 72.5% hit the receiver within a radius of 130 mm (78.7% hit the hexagonal receiver and the remaining 6.3% hit the cavity walls). From the course of the isolines, it can be suggested that the aperture should be placed about 25 mm further away from the concentrator in order to maximize the radiation passing the aperture (87.5% instead of 85%). However, with the given cavity, this would also reduce the part of radiation that directly hits the receiver. Considering only the solar input and ignoring at this point the thermal losses through the opening for better performance, the cavity should therefore be 25 mm shorter and in order to reach 90% intercept, the aperture diameter should be enlarged to 210 mm.

Tracking deviation measurements throughout, an entire day resulted in maximum deviations of -5 ± 11 mm in azimuth and $+4\pm7$ mm in elevation. At the same time, the peak flux density in the absorber plane changed slightly between 1460 kW/m^2 and 1580 kW/m^2.

Power Measurement

Due to its altitude and the clean atmosphere, the site at Odeillo has the particular condition that insolation normally rises very fast

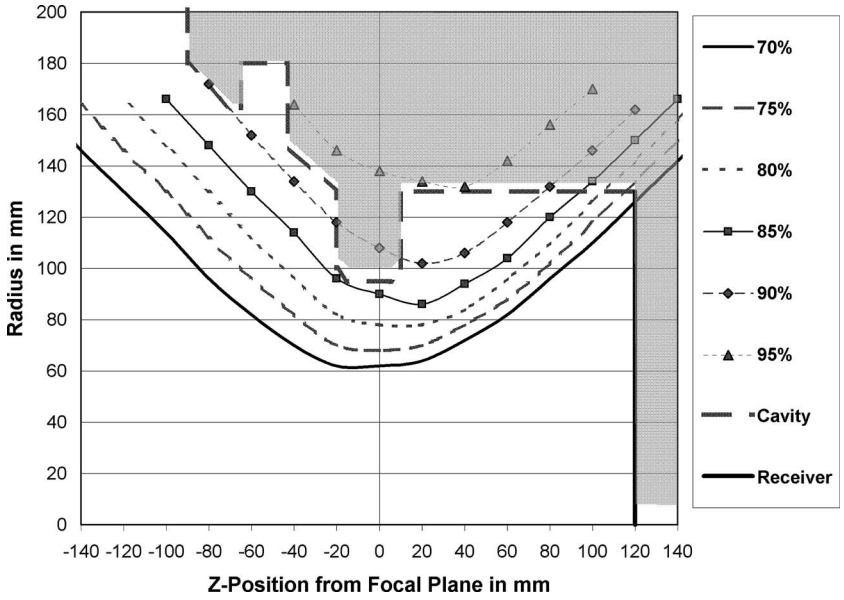

Fig. 6 Intercept radii within the EuroDish cavity

Table 1 Assumptions for simulations

Circular absorber area	0.058 m^2
Cylindrical cavity with radius	136 mm
Cavity aperture radius	95 mm
Homogeneous absorber and cavity wall temperature	850°C
Cavity housing temperature	150°C
Distance from absorber to aperture	120 mm
Directly irradiated length on cavity wall	30 mm
Cavity housing surface area	0.47 m^2
Airspeed inside the package	1 m/s
Surface temperature of engine and oil pan	50°C
Surface area of engine and oil pan	0.7 m^2

to levels where the cooling fan of the receiver starts acting to get rid of the excess heat produced by the oversized concentrator. This introduces an additional, unknown heat flow and makes an exact energy balance impossible. A dish/Stirling system never operates in a perfect steady state since ambient conditions permanently change, and the control system of the engine always works and tries to bring the engine to (or maintain it in) its optimum operation point. The data set was selected to come as close as possible to steady state conditions with negligible changes in the ambient conditions and the engine output parameters [4]. To further reduce the error, 5 min averages of the data were used and are presented in Table 3. Such a representative set of data was compiled in Jan. 19, 2006 at a moderate insolation level of about 900 W/m^2 and low ambient temperature (about −5°C).

Approximation of Additional Cavity Losses

As not all energy flows in the Stirling unit can be measured, calculations have been made to quantify the remaining losses. The considered additional losses include the reflections inside and out of the cavity, IR-radiation losses of receiver, cavity, and the cavity housing, and convection losses of the cavity, the cavity housing, and the Stirling engine surface. For the calculations, some simplifications concerning temperature and flux distribution and the geometrical setup of the system were assumed, as shown in Table 1.

Table 2 Optical material properties

	Absorbance	Reflectance	Emittance at temp.
Receiver (Inconel)	93.0%	7.0%	88.9%
Ceramic insulation	20.0%	80.0%	90.0%

Irradiation properties of the cavity material and the absorber tubes depend on material age and exposure to ambient conditions (e.g., oxide layer, dirt). According to results of measurements taken with similar material samples, they are assumed as shown in Table 2.

The distribution of the reflected light on the different parts of the cavity receiver is calculated assuming Lambertian surfaces with the view factors [5] of all parts to each other. After six reflections, the losses through the cavity aperture change less than 1% and reach a maximum of 1.43 kW.

The radiation losses of the cavity walls and the receiver through the aperture at 850°C are calculated to be 2.6 kW using the view factor model. The convective losses out of the cavity in the orientation it had during the measurements (21 deg facing down) are calculated to be 1.0 kW using the equations given by Leibfried and Ontjohann [6]. The average surface temperature of the cavity housing is around 150°C, which causes IR losses of about 0.33 kW.

Rough calculations for the convective heat losses of the cavity housing and warm engine surfaces were done using simple models of the surfaces and a mixture of free and forced convection caused by the main cooling fan. According to these calculations, the receiver housing contributes with about 0.5 kW and the engine parts with another 0.3 kW to the thermal losses into the STIRLING package.

Energy Balance

The energy balance for the complete system is shown in Table 3 including the calculated precision for measured values as well as estimated errors of the assumptions used in the calculations. At an insolation level of 906 W/m^2 and a reflectance of 92.5%, the dish delivers 44.4 kW of solar radiant power toward the STIRLING package. About 15% of the reflected sunlight does not enter through the aperture. After subtracting the different losses explained above, the total thermal energy transferred to the working gas of the Stirling engine is calculated to be 31.6 kW with an error of ±4.3%.

On the output side of the engine, a total of 30.8 kW output power is calculated by adding shaft and thermal power. Considering the total error of the measurement chain of ±2.9%, this value is consistent within the error bounds of the calculated power input.

Component Efficiencies

From the numbers above, efficiencies for all components can be calculated. Stine and Diver [7] define the concentrator optical ef-

Table 3 Energy balance (errors statistical)

			Comment	Error
Input	Direct normal insolation	906 W/m^2		±1.5%
	Power from dish	44.4 kW	92.5% reflect.; 53 m^2 active area	±1.9%
	Resulting power into aperture	37.75 kW	85% intercept	±3.1%
	Reflection	1.40 kW	Calculated with assumptions	±25%
	Radiation losses	2.59 kW	Calculated with assumptions	±16%
	Convection through aperture	1.00 kW	Calculated with assumptions	±25%
	Radiation and convection into STIRLING package	1.13 kW	Calculated with assumptions	±50%
	Thermal power into engine	31.63 kW	Considering losses above	±4.3%
Output	Electrical output (net STIRLING package)	10.85 kW		±1.0%
	Stirling shaft power	12.25 kW	Considering parasitics and generator efficiency of 92.5%	±1.1%
	Volume flow coolant	4.92×10^{-4} m^3/s		±0.17%
	Coolant density	1060 kg/m^3		±0.5%
	Temperature difference engine out-in	9.94 K		±0.1%
	Heat capacity coolant	3574 J/kg K		±4.0%
	Thermal power out	18.53 kW		±4.0%
	Total power out	30.77 kW		±2.4%

ficiency as the product of unshaded aperture area fraction, reflectance, and intercept factor, which would calculate to 74.4%. The efficiency of the cavity/receiver, i.e., the proportion of the thermal power introduced into the engine to the power that enters the aperture, is 84.5%. The Stirling engine efficiency for the conversion of thermal to mechanical power reaches 39.4% under the given beneficial ambient conditions. This number cannot be applied in general because, as for all thermodynamic converters, it highly depends on the ambient temperature and the efficiency of the cooling system. After subtracting the generator losses of about 7.5% and the consumption of the tracking system (about 100 W), the overall system efficiency for the conversion of solar to net electric power is calculated to be 22.5%.

Conclusions

The approach to establish an energy balance for the 10 kW dish/Stirling system in Odeillo by measuring input and output power of the Stirling engine helped to identify and understand the individual losses of the system components. Since all measurements have a limited precision, the overall error of the balance is quite high. The only error that could have been avoided was the unexpected high uncertainty about the heat capacity of the coolant, which was determined with a specified error of 4%. The campaign was planned for the summer month using water as coolant but was delayed and finally had to be carried out in winter. The authors expected a much higher precision of the coolant analysis through an accepted institution. Errors of the models and assumptions for the calculation of energy transfers that could not be measured directly also had to be assumed very high, as reflected in Table 3.

As we can see in Table 3, almost 30% of the power collected by the concentrator is not transferred into the Stirling cycle. The intercept losses at the aperture lead to the conclusion that the combination of concentrator-aperture can still be optimized. Just looking on the intercept, the aperture diameter should be enlarged by some millimeters but this will have a negative influence on the radiation and convective losses out of the aperture. To reduce all the losses, the optical quality of the concentrator would have to be improved. This might be accomplished by optimizing or changing the manufacturing process of the concentrator segments, which will be the major challenge for further system development.

Acknowledgment

The authors would like to thank N. Boullet (PROMES), T. Keck (SBP), and V. Rümelin (Solo) for their permanent help and comments throughout the campaign. Financial support from the German Ministry for the Environment, Nature Conservation and Nuclear Safety, the French "Agence de l'Environnement et de la Maîtrise de l'Énergie (ADEME)," and the European Commission (SOLFACE program) is gratefully acknowledged.

References

[1] Gineste, J. M., Flamant, G., and Olalde, G., 1999, "Incident Solar Radiation Data at Odeillo Solar Furnaces," J. Phys. IV, **9**, pp. 623–628.

[2] Ulmer, S., 2004, "Messung der Strahlungsflussdichte-Verteilung von Punktkonzentrierenden Solarthermischen Kraftwerken," dissertation, Fortschritt-Bericht VDI Reihe 6 Nr. 510, Düsseldorf.

[3] Ulmer, S., Reinalter, W., Heller, P., Lüpfert, E., and Martínez, D., 2002, "Beam Characterization and Improvement With a Flux Mapping System for Dish Concentrators," ASME J. Sol. Energy Eng., **124**(2), pp. 182–188.

[4] Stine, W. B., 1995, "Experimentally Validated Long-Term Energy Production Prediction Model for Solar Dish/Stirling Electric Generating Systems," *Proceedings of the Intersociety Energy Conversion Engineering Conference*, Orlando, FL, Paper No. 95–166.

[5] VDI-Gesellschaft Verfahrenstechnik und Chemieingenieurwesen, 2006, *VDI Wärmeatlas*, Springer, Berlin.

[6] Leibfried, U., and Ortjohann, J., 1993, *Convective Heat Loss > From Upward and Downward-Facing Cavity Solar Receivers—Measurements and Calculations*, HTC Solar Research GmbH, Lörrach, Germany.

[7] Stine, W. B., and Diver, R. B., 1995, "A Compendium of Solar Dish/Stirling Technology," Sandia National Laboratories Report No. SAND93–7026, Albuquerque, NM.